[2]Kubota, N., and Kuwahara, T., "Combustion of Energetic Fuel for Ducted Rockets (I)," *Propellants, Explosives, Pyrotechnics*, Vol. 16, No. 2, 1991, pp. 51–54.

[3]Kubota, N., Yano, Y., Miyata, K., Kuwahara, T., Mitsuno, M., and Nakagawa, I., "Energetic Solid Fuels for Ducted Rockets (II)," *Propellants, Explosives, Pyrotechnics*, Vol. 16, No. 6, 1991, pp. 287–292.

[4]Hori, K., and Kimura, M., "Combustion Mechanism of Glycidyl Azide Polymer," *Propellants, Explosives, Pyrotechnics*, Vol. 21, No. 3, 1996, pp. 160–165.

[5]Menke, K., and Eisele, S., "Rocket Propellants with Reduced Smoke and High Burning Rates," *Propellants, Explosives, Pyrotechnics*, Vol. 22, No. 3, 1997, pp. 112–119.

[6]Marinkas, P. L. (ed.), *Organic Energetic Compounds*, Nova Science Publishers, New York, 1996, pp. 47–163.

[7]Pfeil, A., and Lobbecke, S., "Controlled Pyrolysis of New Energetic Binder Azide Polyester PAP-G," *Propellants, Explosives, Pyrotechnics*, Vol. 22, No. 3, 1997, pp. 137–142.

[8]Sahu, S. K., Panda, S. P., Thakur, J. V., Kulkarni, S. G., Kumbhar, C. G., and Sadfule, D. S., "Synthesis and Characterization of Hydroxy Terminated Polyepichlorohydrin and Polyglycidyl Azide," *Defence Science Journal*, Vol. 46, No. 5, 1996, pp. 399–403.

[9]*Military Explosives*, Chemical Manual, TM 9-1910/TO 11A-1-34, Departments of the Army and the Air Force, Washington 25, DC, 14 April 1955, pp. 43–49.

[10]Chen, J. K., and Brill, T. B., "Thermal Decomposition of Energetic Materials 548. Kinetics and Near Surface Products of Polymers AMMO, BAMO and GAP in Stimulated Combustion," *Combustion and Flame*, Vol. 87, No. 2, 1991, pp. 157–168.

[11]Sahu, S. K., Panda, S. P., Sadafule, D. S., Kumbhar, C. G., Kulkarni, S. G., and Thakur, J. V., "Thermal and Photodegradation of Glycidyl Azide Polymer," *Polymer Degradation and Stability*, Vol. 62, No. 3, 1998, pp. 495–500.

Numerical Simulation of Axisymmetric Solid Rocket Motor Ignition Transient with Radiation Effect

In Hyun Cho*
Korea Aerospace Research Institute, Yusung-ku, Taejon, 305-600, Republic of Korea
and
Seung Wook Baek†
Korea Advanced Institute of Science and Technology, Gusung-dong, Yusung-ku, Taejon 305-701, Republic of Korea

Introduction

THE solid rocket ignition transient representing a short period right after starting the rocket motor consists of propellant ignition, flame spreading, and chamber filling/pressurization. High-temperature and high-pressure gases ejected from the ignitor at the fore-end section of the rocket chamber heat up the solid propellants. As the heat flux to the propellant surface increases, the propellant starts to burn and releases a large amount of thermal energy in the combustion chamber. Propellant ignition is begun at the head end of the chamber, and the flame spreads toward the end of the rocket, finally burning along the whole propellant surface. The detailed analysis of this ignition transient phenomenon is very important to the efficiency and safety of the solid rocket motor. Inside the rocket motor, radiation is considered to affect the thermal characteristics that will finally change the fluid dynamics. However, its analysis presents a formidable challenge inasmuch as the radiative transfer equation (RTE) is a form of integro-differential equation. Even if there were numerous methods to solve the RTE, the recently proposed finite volume method[1] is considered a good choice for application because this method can easily be applied to complex geometries and be coupled with the other discritized equations.

In this study a more refined model is developed to examine the ignition transient in an axisymmetric solid rocket motor by solving an unsteady turbulent flowfield. In contrast to previous studies,[2,3] the effects of gas radiation are taken into account. Whereas the radiative transfer equation is solved using the finite volume method, the other governing equations are numerically solved using the SIMPLER algorithm in generalized coordinates.

Mathematical Model

Conservation Equations

When the ignitor located at the center of the port is activated as shown in Fig. 1a, the ejected plume starts momentum and heat transfer to the solid propellant. The Favre averaged, two-dimensional axisymmetric Navier–Stokes equations with k–ε turbulent transport model governing this turbulent transport phenomena are developed as follows.

Mass:

$$\frac{\partial \bar{\rho}}{\partial t} + \frac{\partial}{\partial x_i}(\bar{\rho}\tilde{u}_i) = 0 \tag{1}$$

Momentum:

$$\frac{\partial}{\partial t}(\bar{\rho}\tilde{u}_i) + \frac{\partial}{\partial x_j}\left(\bar{\rho}\tilde{u}_i\tilde{u}_j - \mu_{\text{eff}}\frac{\partial \tilde{u}_i}{\partial x_j}\right) = -\frac{\partial \bar{p}}{\partial x_i} + \frac{\partial \tau_{ij}}{\partial x_j} \tag{2}$$

Energy:

$$\frac{\partial}{\partial t}(\bar{\rho}\tilde{h}) + \frac{\partial}{\partial x_j}(\bar{\rho}\tilde{u}_j\tilde{h}) = \frac{\partial \bar{p}}{\partial t} + \tilde{u}_j\frac{\partial \bar{p}}{\partial x_j} - \nabla\cdot q - \nabla\cdot q^r + \Phi \tag{3}$$

Laminar and turbulent heat flux:

$$q = -\left(\frac{\mu_l}{Pr_l} + \frac{\mu_t}{Pr_t}\right)\frac{\partial \tilde{h}}{\partial x_j} \tag{4}$$

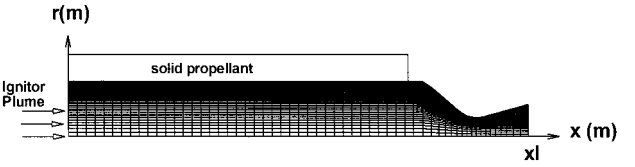

a) Grid system

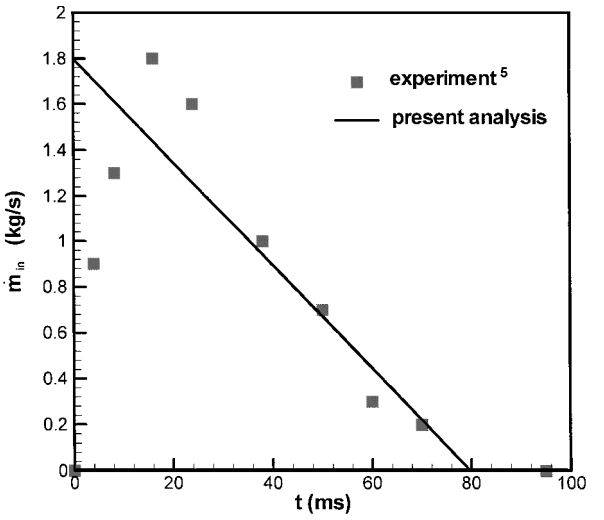

b) Ignitor plume mass flow rate $\dot{m}_{\text{in}}$

Fig. 1 Grid system and mass flow rate by ignitor.

Received 3 June 1996; revision received 16 October 1999; accepted for publication 26 October 1999.

*Senior Researcher, Department of Space Propulsion System.

†Professor, Department of Aerospace Engineering. Senior Member AIAA.

State:

$$\bar{p} = \bar{\rho} R_u \tilde{T} \tag{5}$$

Turbulent kinetic energy:

$$\bar{\rho}\frac{\partial k}{\partial t} + \bar{\rho}\bar{u}_i\frac{\partial k}{\partial x_i} = \frac{\partial}{\partial x_i}\left[\left(\mu_l + \frac{\mu_t}{\sigma_k}\right)\frac{\partial k}{\partial x_i}\right] + P_t - \bar{\rho}\varepsilon \tag{6}$$

Dissipation:

$$\bar{\rho}\frac{\partial \varepsilon}{\partial t} + \bar{\rho}\bar{u}_i\frac{\partial \varepsilon}{\partial x_i} = \frac{\partial}{\partial x_i}\left[\left(\mu_l + \frac{\mu_t}{\sigma_\varepsilon}\right)\frac{\partial \varepsilon}{\partial x_i}\right] - C_1\frac{\varepsilon}{k}P_t - C_2\bar{\rho}\frac{\varepsilon^2}{k} \tag{7}$$

Eddy viscosity:

$$\mu_t = \bar{\rho} C_\mu (k^2/\varepsilon) \tag{8}$$

The model includes six empirical constants, typical values of which are[2]

$$\sigma_k = 1.0, \qquad \sigma_\varepsilon = 1.3, \qquad C_1 = 1.44$$
$$C_2 = 1.92, \qquad C_\mu = 0.09 \tag{9}$$

By taking into account of the sublayer effect, the turbulent Prandtl number Pr_t is defined by[4]

$$Pr_t = 1 \Bigg/ \left\{\frac{1}{2Pr_{t\infty}} + CPe_t\sqrt{\frac{1}{Pr_{t\infty}}} - (CPe_t)^2\left[1 - \exp\left(-\frac{1}{CPe_t\sqrt{Pr_{t\infty}}}\right)\right]\right\} \tag{10}$$

where Pe_t is a turbulent Peclet number, $Pr_{t\infty}$ (=0.85) is the local value of Pr_t at a position far from the wall, and C(=0.3) is an experimentally determined constant.

The two-dimensional heat conduction equation is used to obtain the temperature field of the propellant:

$$\rho_s C_s\frac{\partial T_s}{\partial t} = \frac{\partial}{\partial x_j}\left(\lambda_s\frac{\partial T_s}{\partial x_j}\right) \tag{11}$$

where the subscript s denotes a property of solid propellants. C_s and λ_s have values of 860 J/kg K and 1.85 W/m K, respectively.

Initial and Boundary Conditions

The inlet simulates the ignitor exit conditions, for which stagnation conditions are given by[5]

$$P_{\text{ig}}^0 = 100 P_{\text{atm}}, \qquad T_{\text{ig}}^0 = 2520\ \text{K} \tag{12}$$

Corresponding static conditions for the ignitor plume can be calculated by

$$V_{\text{in}} = \dot{m}_{\text{in}}/A_{\text{in}}\rho_{\text{in}}, \qquad \rho_{\text{in}} = P_{\text{ig}}^0 \Big/ R_{\text{ig}}^0 T_{\text{ig}}^0$$
$$T_{\text{in}} = T_{\text{ig}}^0 - 0.5\left(V_{\text{in}}^2 \Big/ C_{P_{\text{in}}}\right) \tag{13}$$

At the solid propellant surface, the boundary conditions for energy below autoignition temperature are as follows, with the subscript P denoting propellant surface properties:

$$-\lambda\frac{\partial T}{\partial r}\bigg|_P - q_P^r - \rho_s v_P Q_s|_P = -\lambda_s\frac{\partial T_s}{\partial r}\bigg|_P \tag{14}$$

The right-hand side of Eq. (14) represents the inward conductive heat flux away from propellant surface. Whereas the second term on the left-hand side is a radiative heat flux toward the propellant surface, the first and third terms are the conductive heat flux into the propellant surface and the net heat release due to surface reaction. Here ρ_s is solid propellant density (=1728 kg/m^3) and Q_s is the heat of reaction due to surface reaction (=1.05 $\times 10^3$ kJ/kg). The surface temperature $T_{S,P}$ is determined through the aforementioned interface conditions. The burning rate of solid propellant is calculated using the following relation[6]:

$$v_p = v_{p,\text{ref}}(P/P_{\text{ref}})^n + \alpha_e G^{0.8} D_h^{-0.2}\exp(-\beta_e v_p \rho_p/|G|) \tag{15}$$

where $G = \rho u$, D_h is the hydraulic diameter, α_e =6.5 cm$^{2.8}$/g$^{2.8}$s$^{0.2}$, β_e =125, $v_{p,\text{ref}}$ =1.47 cm/s, P_{ref} =68.08 atm, and n =0.44. Once the propellant surface reaches the autoignition temperature (620 K), a burned gas with flame temperature 2968 K (Ref. 5) is considered to be supplied to the gas phase at the propellant surface as a boundary condition. At the axis of symmetry, axisymmetric boundary conditions are applied. At the exit, atmospheric conditions are used if the flow is subsonic, and the solution is extrapolated if the flow is supersonic.

Radiative Heat Transfer

The radiation has an influence on the propellant, both the divergence term of the energy equation and the boundary condition. For a gray medium, the divergence of radiative heat flux is evaluated from

$$-\nabla\cdot q^r = a\left[-4\pi I_b(\boldsymbol{s}) + \int_{4\pi} I(\boldsymbol{s}, \boldsymbol{\Omega})\,\mathrm{d}\omega\right] \tag{16}$$

where a is the absorption coefficient, I_b is the blackbody intensity, $\boldsymbol{\Omega}$ is the direction of radiation, and $I(\boldsymbol{s}, \boldsymbol{\Omega})$ is the directional intensity.

To find $I(\boldsymbol{s}, \boldsymbol{\Omega})$, we solve the radiative heat transfer equation for gray gas,

$$\frac{\mathrm{d}I(\boldsymbol{s}, \boldsymbol{\Omega})}{\mathrm{d}s} = -(a + \sigma_s)I(\boldsymbol{s}, \boldsymbol{\Omega}) + aI_b(\boldsymbol{s}) + \frac{\sigma_s}{4\pi}\int_{\Omega' = 4\pi} I(\boldsymbol{s}, \boldsymbol{\Omega}')\Phi(\boldsymbol{\Omega}', \boldsymbol{\Omega})\,\mathrm{d}\omega \tag{17}$$

where σ_s is the scattering coefficient and $\Phi(\boldsymbol{\Omega}', \boldsymbol{\Omega})$ is the scattering phase function.

A diffusely emitting and reflecting surface condition on the propellant and nozzle wall surface is applied. Surface emissivity is assumed to be 0.5.

Results and Discussion

The governing equations are transformed into generalized form and can be discretized into the algebraic form and solved by the compressible SIMPLER algorithm.[7] The global iterations are continued until the maximum mass residual becomes less than 10^{-4}. The time step is 0.1 ms and Courant–Friedrichs–Lewy number used is close to 1.

Metalized propellant has a greater radiation effect than nonmetalized propellant, but the main purpose of this research is to show the gas radiation effect on the chamber flowfield. Therefore, nonmetalized propellant is assumed, and the effect of radiation is taken into account with an absorption coefficient of 50 m^{-1}, while the scattering effect is ignored. A nonuniform grid system of 70 $\times$ 40 in the gas phase and 50 $\times$ 10 in the solid propellant, as shown in Fig. 1a, was used. An experimental ignitor plume mass flow rate $\dot{m}_{\text{in}}$ is plotted in Fig. 1b.[5] For the present numerical analysis, the mass flow rate is simplified as a linear profile.

In Fig. 2a the temporal variation of head-end pressure is plotted for a =50 m^{-1} and without radiation. The numerical results for a =50 m^{-1} predict the experimental data reasonably well, whereas the case without radiation does not accurately predict the head-end pressure variation. This results because there is more heat feedback to the propellant surface for the case with a =50 m^{-1}, so that both the propellant surface temperature and the propellant burning rate increase. On the other hand, the case without radiation underpredicts the head-end pressure because there is less heat feedback to the propellant. Figure 2b compares the propellant surface temperature distribution. With radiation, the whole propellant surface is ignited

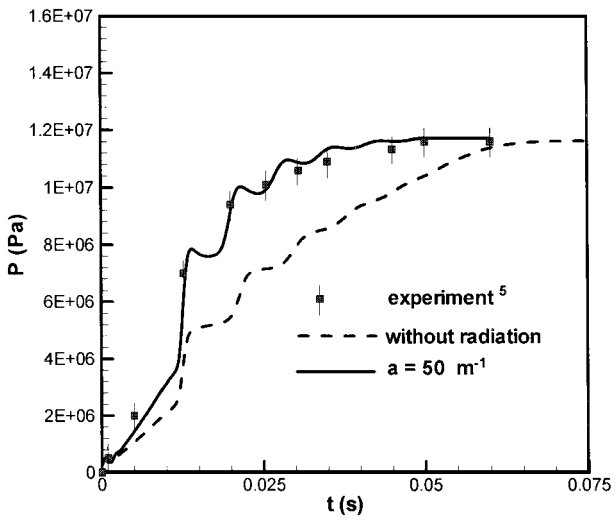

a) Temporal head-end pressure

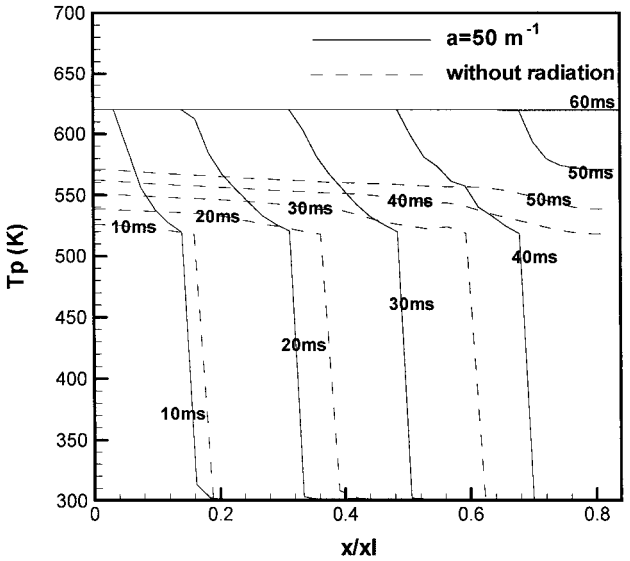

b) Temporal propellant surface temperature

Fig. 2 Temporal head-end pressure and propellant surface temperature.

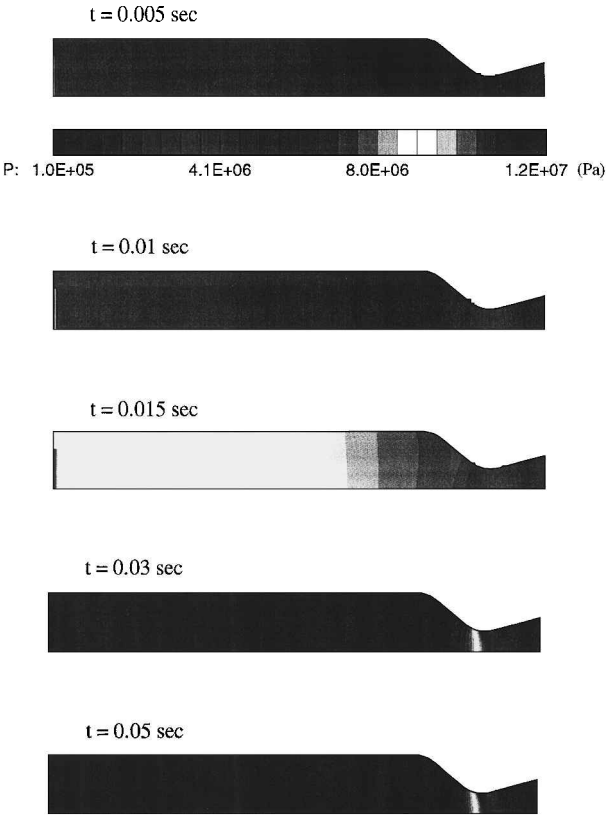

Fig. 3 Temporal variation in pressure.

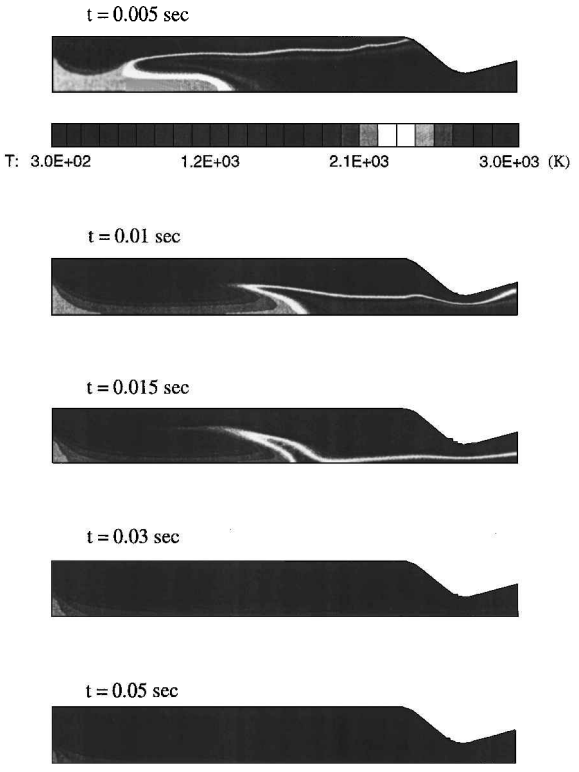

Fig. 4 Temporal variation in temperature.

at 60 ms, and flame spreading is accomplished. Without radiation, energy transfer from the ignitor gas to the propellant continues, but the propellant surface is not completely ignited until 500 ms.

Unsteady pressure distribution is shown in Fig. 3. Compression waves generated by the ignitor pass the midzone at about 5 ms in Fig. 3. A chamber filling procedure will probably be completed at about 50 ms. Flow expansion is also clearly shown in the converging and diverging nozzle sections.

A contour of the temporal variation in gas phase temperature is plotted in Fig. 4. In Fig. 4, the flame spreading is shown to be complete at about 5 ms, and by this time the entire propellant surface is burning. Because radiation is included, the flame spreading is seen to be faster than the case without radiation, which is not included here for the sake of brevity.

Conclusions

In this study, the applicability of numerical procedures to the analysis of the ignition transient in the solid rocket motor has been investigated. In particular, the effect of radiation on internal flow development was taken into account. Heat transfer from the gas to the propellant surface by radiative and convective heat transfer raises the surface temperature and burning rate. Radiation plays a significant role in igniting the solid propellant by enhancing the heat feedback to the propellant surface because relatively long ignition delay is required without radiation.

Acknowledgment

We are very grateful for financial support from the Agency for Defense Development.

References

[1]Chai, J. C., Parthasarathy, G., Lee, H. S., and Patankar, V., "Finite Volume Radiative Heat Transfer Procedure for Irregular Geometry," *Journal of Thermophysics and Heat Transfer*, Vol. 9, No. 2, 1995, pp. 410–415.

[2]Bai, S. D., Han, S. S., and Pardue, B. A., "Two-Dimensional Axisymmetric Analysis of SRM Ignition Transient," AIAA Paper 93-2311, 1993.

[3]Johnston, W. A., "Solid Rocket Motor Internal Flow During Ignition," *Journal of Propulsion and Power*, Vol. 11, No. 3, 1995, pp. 489–496.

[4]Kays, W. M., and Crawford, M. E., *Convective Heat and Mass Transfer*, McGraw–Hill, New York, 1993.

[5]Chang, S. T., and Cha, H. S., "Ignition Tests of Small Solid Rocket Motor," ADD Rept. MSDC-421-940099, 1994.

[6]Caveny, L. H., and Kuo, K. K., "Ignition Transients of Large Segmented Solid Rocket Boosters," NASA CR-150162, 1976.

[7]Karki, K. C., and Patankar, S. V., "Pressure-Based Calculation Procedure for Viscous Flows at All Speeds in Arbitrary Configurations," *AIAA Journal*, Vol. 27, No. 1, 1989, pp. 1167–1175.